PAPER

Redox mediated photocatalytic water-splitting in optofluidic microreactors

Syed Saad Ahsan,[a] Abdurrahman Gumus[b] and David Erickson*[c]

While photocatalytic water-splitting is a promising alternative energy source, low photocatalytic efficiencies in the visible spectrum hinders its widespread deployment and commercialization. Although screening combinations of new materials and characterizing their reaction kinetics offers possible improvements to efficiency, current experiments are challenged by expensive bulky setups and slow recovery of particles downstream. Optofluidics is a good platform for screening Z-scheme catalysts cheaply and rapidly. By alleviating the problems of mass transport it can also potentially increase reaction rates and efficiencies. Here, we demonstrate a novel optofluidic device based on applying catalyst sol-gels on planar channels while measuring the reaction output by monitoring the depletion of the redox mediators. We use our setup to study the kinetics of the TiO_2–Pt water-splitting reaction mediated by I^-/IO_3^- redox pairs under different flow rates. In particular, for TiO_2–Pt, we show ~2-fold improvements in reaction rates and efficiencies.

Introduction

With fossil fuels contributing about 85–90% of the global demand for energy,[1] there is dire need for alternative sources of energy that are both sustainable and environmentally-friendly. One possible alternative is the solar energy that falls on the surface of the earth. More energy arrives on the surface of the earth in one hour than the global yearly demand for energy in 2005.[2] Unfortunately, the intermittency of solar illumination and the storage and transport of the resulting energy remains a difficult challenge. Using fuels produced by solar-chemical reactions, such as hydrogen from photocatalytic water-splitting, could replace the use of fossil fuels with little change to the current energy infrastructure and without the undesirable carbon dioxide emissions.

For solar-driven photocatalysis, the relevant variable for semiconductors is the bandgap energy which determines the wavelength above which the semiconductor will not form electron-hole pairs and thus will not catalyze the reaction, and the photo-conversion efficiency which is relevant for prospects of commercializing the technology. Some of the promising applications of photocatalysis are in water treatment,[3] air pollution,[4] self cleaning, disinfection[5] and water-splitting. While photocatalytic water-splitting is not new,[6] current technology has not been able to meet the stated goals of

30% quantum yield at 600 nm which corresponds to 5% solar energy conversion.[7]

There are many strategies to enhance the photocatalytic water-splitting efficiency and cut-off wavelength such as noble-gas doping, co-catalyst impregnation, noble-metal loading, plasmonic sensitization, and employing wire or belt-shaped geometries as described by Tong *et al.*[8] Another popular strategy is to employ a Z-scheme system. In this scheme, oxygen and hydrogen are evolved at different catalysts, while redox mediators, such as iodide/iodate pairs, serve as the oxidizing or reducing agents as in Fig. 1(a). Because the water-splitting reaction is ultimately performed using two photons as opposed to one, the demand on each side of the reaction is lessened allowing for higher efficiencies at larger wavelengths. The highest values for quantum efficiency under visible light without using a sacrificial reagent are reported using a ZrO_2/TaON and Pt–WO_3 Z-scheme system.[9]

Because optofluidics combines fluids and their interaction with light, it is potentially the optimal platform for photocatalytic reactions[10] and can increase reaction rates by improving mass and optical transfer efficiencies.[11] Additionally, by miniaturizing the reactor space, one may minimize the requirements for time, reagents and equipment. These requirements are often significant for current water-splitting setups. At present, experiments are typically run in large closed volume setups with catalysts suspended in the solution, constantly bubbled with nitrogen gas and attached to a gas chromatograph to monitor the output products.[7] Because of the large setup, the material constraints for preparing the catalyst are not trivial. The photo-catalysts are generally recovered downstream using centrifuges and filters,

[a]*Applied and Engineering Physics, Cornell University, Ithaca, NY, 14853, USA*
[b]*Electrical and Computer Engineering, Cornell University, Ithaca, NY, 14853, USA*
[c]*Sibley School of Mechanical and Aerospace Engineering, Cornell University, Ithaca, NY, 14853, USA. E-mail: de54@cornell.edu*
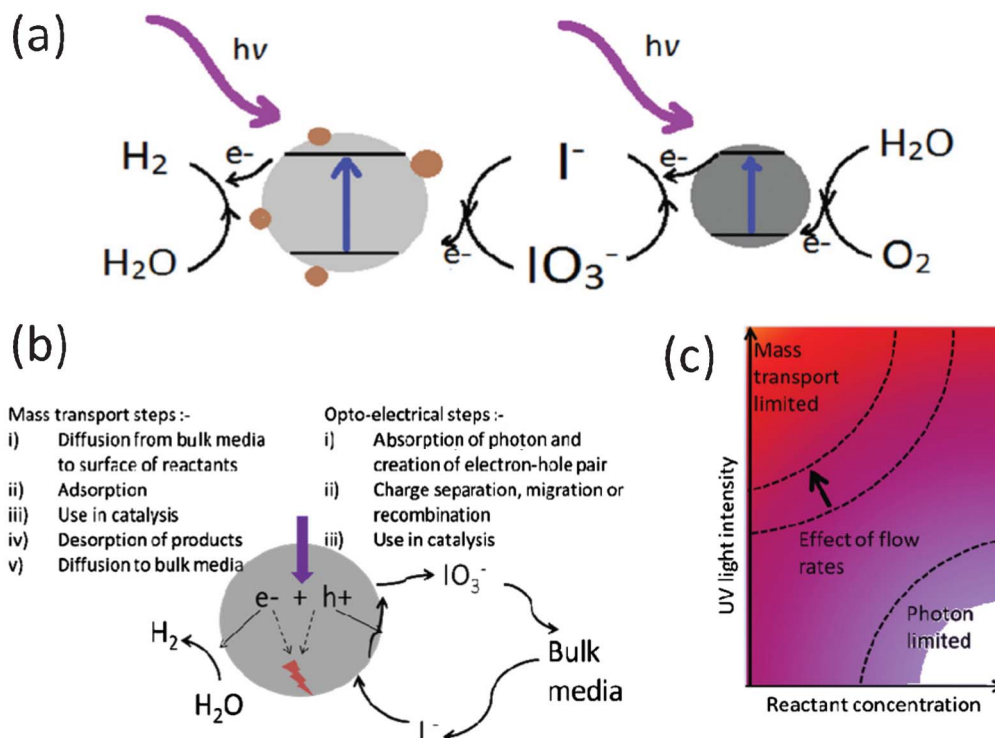
Fig. 1 Illustration of chemical reaction, reaction steps, and important kinetic regimes. **(a)** An illustration of a Z-scheme system where a redox mediator pair couples to the two different reactions. **(b)** A closer look at the reaction steps. For the opto-electrical step, the photon gets absorbed creating an electron-hole pair, which either recombines or separates and proceeds to catalyze the reaction. In the mass-transport step, the reactants and the products have to not only diffuse to the surface but also adsorb and desorb during the reaction. **(c)** A rough sketch of the interesting kinetic regimes where the reaction is photon-limited (has the highest quantum efficiency) and mass-transport limited (where the reaction output is capped). Please refer to cited literature.[14]

washed and then reused in the setup for experiments under different conditions.[12,13] Another advantage of optofluidic reactors is that they allow for different experiments to be conducted rapidly because the catalysts can be washed and reused for experiments with different input reagents. This allows for rapid optimization of reaction conditions and study of the kinetic properties. Additionally, while the highest reported quantum efficiencies were achieved by optimizing the reaction conditions,[9] the kinetics of water-splitting reactions under a broad range of conditions has not been studied. While there have been a few comprehensive kinetics studies that have been performed on photocatalysis for exothermic reactions, such as degradation reactions,[14] there have been no satisfactory comprehensive kinetic studies for truly complex endothermic reactions like water-splitting.

We can reasonably discern that all photocatalytic reactions happen in two steps[14] as in Fig. 1(b). In the first step, the photon is absorbed by the semiconductor particle creating an electron-hole pair which either recombines or travels to the surface of the particle to catalyze the reaction of interest. This first-step which can be improved through chemistry and material science determines the ultimate limit of the photo-catalytic efficiency. The second step involves the removal of the products and the introduction of new reactants to the catalyst site. This mass transport step is important to ensure the adequate presence of reactants on the catalyst surface and

for endothermic reactions, like water-splitting, the speedy removal of products to avoid reverse reactions. The opto-electrical transport and mass transport steps determine regimes of interest in photocatalysis which are illustrated in Fig. 1(c). At low levels of illumination to reactant concentrations, the reaction is photon-limited at which point it has the highest photocatalytic efficiency for a given catalyst chemistry. At high levels of illumination of reactant concentration, the reaction is mass-transport limited. Indeed, there have been many studies showing improvement of catalytic output (for reactions other than water-splitting) inside optofluidics as opposed to conventional plate and slurry reactors[11,15–17] due to superior mass transport. Although the improved mass transport may help in removing product gas molecules, it is hard to imagine single-photon water-splitting being mass-transport limited in aqueous solutions when the reactant is water itself; however, it is much easier to see how a Z-scheme system could potentially be mass-transport limited. Indeed, because it is not possible to improve the ultimate photon-limited efficiency by changing reaction conditions as has been accomplished in previous studies,[9] we suggest that in Z-scheme systems improving mass transport could potentially yield significant improvements in photo-catalytic efficiency.

While others have studied photocatalysis of degradation reactions on similar optofluidic platforms,[11,18] we demonstrate the first optofluidic system to study the kinetics of

photocatalytic water-splitting for TiO_2–Pt catalyst mediated by I^-/IO_3^- redox pairs. Like others,[11,15–17] we demonstrate that optofluidics, by alleviating the problems of mass transport, can increase reaction rates and efficiencies. Additionally, we believe that such a platform could also allow for cheap and rapid system optimization and catalyst pre-screening. We suggest that optofluidics may not only enable higher reaction rates and efficiencies but would also be the ideal environment to study water-splitting photocatalysis.

Materials and methods

To maximize the light-collection area, a planar reactor space was chosen. A schematic of our device is shown in Fig. 2(a). Our channels were fabricated using thin parafilm that could be used to create devices rapidly and bind glass to glass. We avoided PDMS as it absorbs UV light and has an insufficient elastic modulus required for stability in such a planar design. To apply the sol–gel on the glass slide, we covered the glass slide with tape and then cut out a rectangular area of 3.75 cm by 1.25 cm. 50 μL of the sol–gel were then taken and applied to the glass slides and distributed to create a microfilm. The glass slides were then dried for 2 h at 80 °C after which they were calcinated at 550 °C for 6 h in a controlled atmosphere furnace in air to create a thin film on the surface as shown in Fig. 2(b).
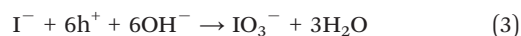
To create the Pt–TiO_2 sol–gel, a dispersed colloidal suspension of platinum particles was first made by reducing hexachloroplatinic acid in borohydride in a solution with 1% PVP. The suspension was slowly dried to concentrate the platinum particles to 70 mL of solution. Then 0.23 mL of acetylacetone was added and thoroughly mixed. Then 7 g anatase TiO_2 nanopowder (50 nm size from Sigma Aldrich) was slowly added and mixed to disperse the powder over the solution. Then 0.2 mL of a Triton X-100 was added to facilitate the spreading of the colloid after which 1.4 g of polyethylene glycol was added into the solution. The solution was then left to mix overnight and was ready to use afterwards.

We used a 100 W Hg lamp in our experiments. The input solution was kept at pH 12 by adding NaOH to ensure that we would not produce tri-iodide species and to ensure that the depletion in iodine species corresponded to oxygen and hydrogen production as previously reported.[19] To calibrate the output of our reaction, we collected the output of the reaction solution in the microreactor both before and after we illuminated our microreactor with the UV light to take into account possible contamination by displaced catalyst particles. The output samples were then taken to a UV-Vis absorption spectrophotometer where we looked at the absorption spectrum from 200–260 nm. The absorption spectrophotometry fit the Beer–Lambert law in the control measurements for different proportions of iodide to iodate as in Fig. 3(a). Additionally, iodide and iodate have different peaks in the UV region making it possible to confirm the reaction using spectrophotometric evidence as well, as is shown in Fig. 3(b). All iodine concentrations higher that 200 μM were diluted to 200 μM before being analyzed by absorption spectrophotometry.

Results and discussion

As described by others,[7,9,19] the equations of the water-splitting reactions redox mediated by I^-/IO_3^- pairs are:

$$IO_3^- + 6e^- + 3H_2O \rightarrow I^- + 6OH^- \tag{1}$$

$$4OH^- + 4h^+ \rightarrow O_2 + 2H_2O \tag{2}$$

$$I^- + 6h^+ + 6OH^- \rightarrow IO_3^- + 3H_2O \tag{3}$$

$$2H^+ + 2e^- \rightarrow H_2 \tag{4}$$

Because we monitor the reaction rates *via* the depletion of the redox mediators, one possible limitation for our device to study photocatalysis is the requirement that the catalyst being studied is reaction specific. If the catalyst can carry out both the oxygen-producing reaction and the hydrogen-producing reaction, then the photo-production of oxygen and hydrogen may not be correlated with the depletion of the respective redox pairs and our method cannot be used adequately. However, most catalysts that are developed for Z-scheme systems are specific for each side of the reaction and the depletion of the redox pairs is correlated with the production of oxygen and hydrogen. In addition, even if the catalyst can carry out both sides of the reaction, depletion of redox mediators may still be used if the photocatalyst is reaction specific in the kinetic regimes that are studied.

In fact, in our experiments we used a catalyst that catalyzes both sides of the reaction. However, we used information from
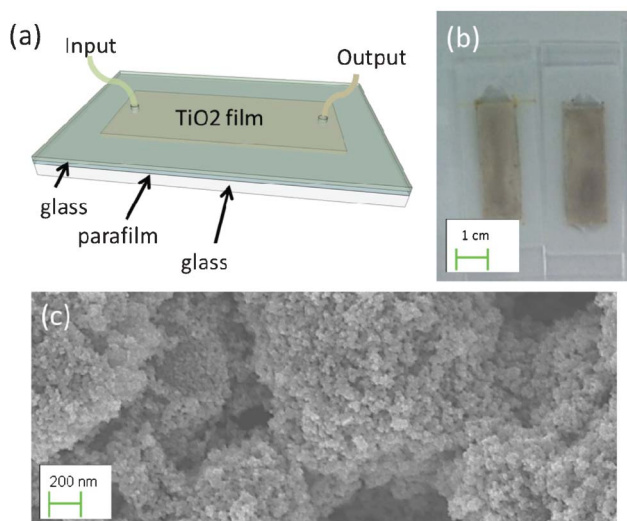

Fig. 2 Fabricated device, and SEM of thin film. (a) Schematic of parafilm device. (b) Thin TiO_2 films. The two slides on the left are impregnated with Pt (0.3%). (c) SEM of thin film shows porous structure with high surface to volume ratio.
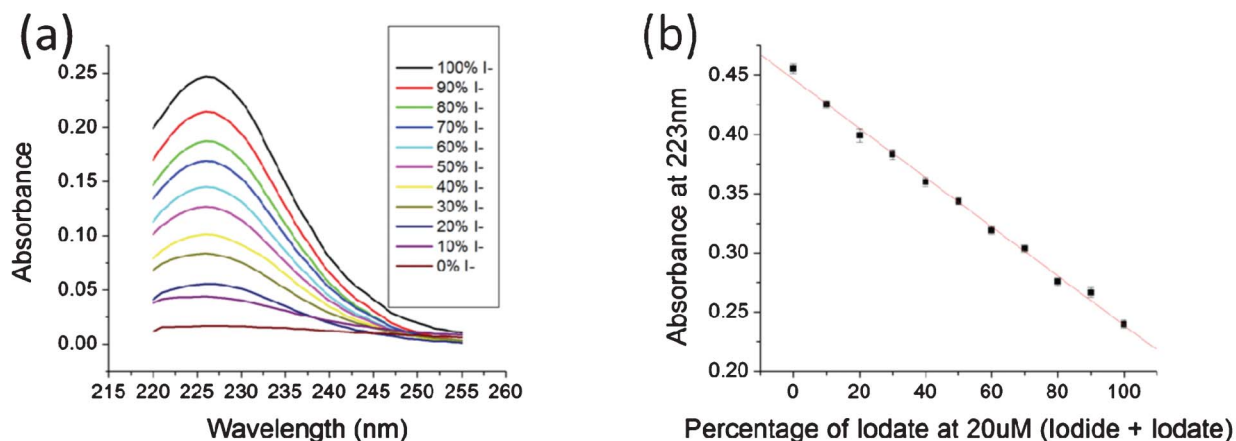
Fig. 3 Absorbance spectra of iodide/iodate and fit. **(a)** Absorbance spectra for different proportions of iodide in 20 μM (iodide + iodate) solution normalized against buffer. **(b)** Using the Beer–Lambert law, $A = \varepsilon c l$, we were able to discriminate 20 μM of iodine species of different proportions with an error of 1.4%.

previous studies to make sure the regimes we studied were reaction-specific. According to previous literature,[19] the Pt–TiO₂ catalyst is reaction specific for the oxygen-producing reaction (1) + (2) when the concentration of iodate is high, and specific for the hydrogen-producing reaction (3) + (4) (albeit with its corresponding reverse reactions) at very high iodide concentrations. As a result, the depletion of the iodine species corresponds to the production of hydrogen/oxygen in the regimes that we studied.

To assess the functionality of our microreactor, we confirmed that the reaction remained constant over a long period of time which we show in Fig. 4. To do this, we introduced 200 μM pure iodate solution at 100 μL min⁻¹ over the course of 90 min under the presence of UV light. Our results showed that the reaction output remained constant over this period which was longer than in previous studies that found the iodine species disabled the catalyst after 30 min.[20]

Additionally, we found that in our microfluidic chip we were able to self-clean the catalyst allowing us to change the input reagents after the cleaning and to try different concentrations or species. This showcases the advantage of carrying out these reactions in an optofluidic chip as opposed to in a bulk reactor because we could forgo the time-consuming steps of recovery, cleaning and reintroduction.

We also measured the reaction rates for the oxygen producing reaction under different flow rates to check for the effect of improved mass transfer efficiency. To do this, we introduced different concentrations of NaIO₃ solution at pH 12 to the input. Our results, shown in Fig. 5(a), indicate that there is clearly an improvement in reaction efficiency at higher flow rates. We believe like in previous studies,[11] that this is due to the improvement in the reaction rate due to improved mass transport. Additionally, we also studied the reaction kinetics of the hydrogen producing reaction under different flow rates. To
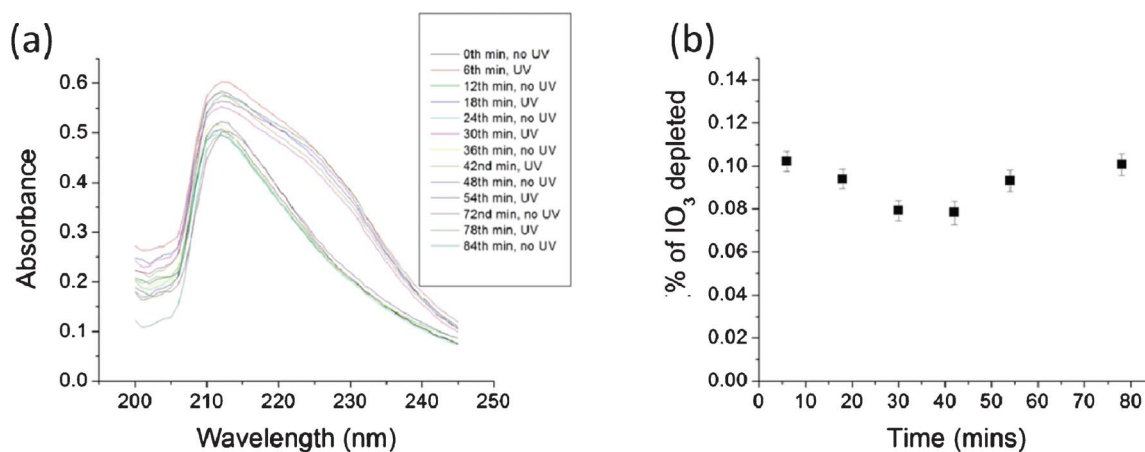

Fig. 4 Plots of catalytic activity over time. **(a)** Absorbance spectrum of the output of the reactor at a flow rate of 100 μL min⁻¹ for input of 200 μM iodate. UV light was toggled on and off every 6 min for a span of 90 min. **(b)** Photocatalytic activity measured by iodate depletion in reactor. The output remains constant over the entire 90 min period.
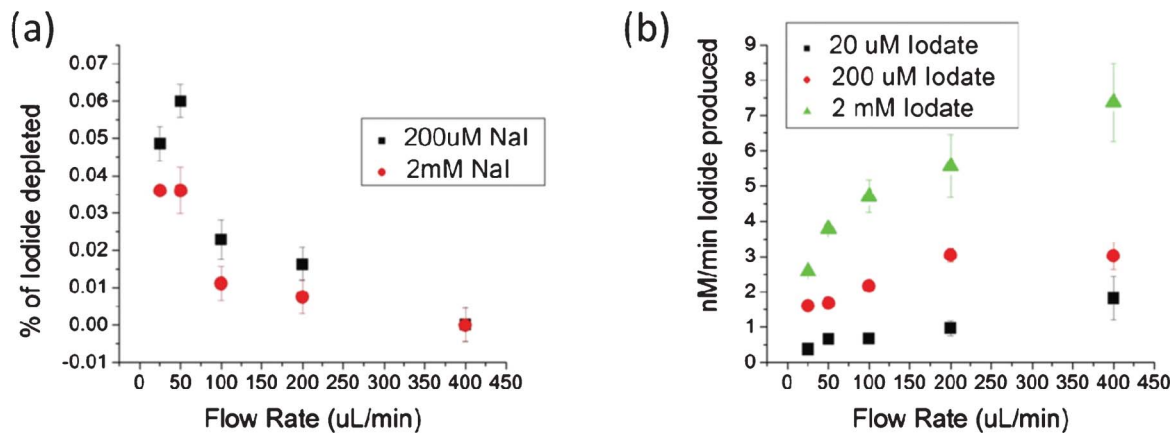
Fig. 5 Plots of catalytic activity at different flow rates. **(a)** Photocatalytic activity for hydrogen-producing reaction in reactor. The maximum percentage conversion of iodide to iodate is capped at $5 \pm 1\%$. Increasing the flow rates improves the output. The reaction is severely mass-transport limited at $25~\mu L~min^{-1}$ from 20 μM NaI to 2 mM NaI where activity increases proportionally to concentration. **(b)** Catalytic output for oxygen-producing reaction. Increasing the flow rates clearly increases the output.

do this, we introduced different concentrations of NaI solution at pH 12. We found that the output concentration was always capped such that the amount of iodide catalyzed to iodate would never increase above a certain proportion of the concentration as is shown in Fig. 5(b). For low concentrations of iodide, the proportion of iodide catalyzed to iodate was capped at $5 \pm 1\%$. This agrees with results presented in previous literature[19] that found a high iodide concentration equilibrium presumably due to the better adsorption of the iodate species on the titanium oxide surface. Syncing the two systems together shows that at comparable reaction rates, simply increasing flow rates would amount to at least ~2-fold improvement in the reaction rate and efficiency.

While mass transport can also be improved by increasing the concentration of the reactants (in our case the redox mediators) as shown here and noted in previous studies,[14] there is also a visible proportional improvement across the concentrations that we studied, clearly seen for the oxygen-producing reaction, which we believe comes not from the introduction of new reactants to the catalyst site but from the removal of the products to decrease the possibility of the reverse reaction. Additionally, it is not always suitable to increase the concentration of reactants for prospects of commercialization, especially for the iodide/iodate redox pairs, due to their corrosive and toxic nature at higher concentrations.

Part of the improvement in reaction rates at higher flow rates come from improved mass transport. These improvements are consistent with previous experiments and have often been explained with the use of the following equation:[11]

$$\frac{1}{k} = \frac{1}{KL} + \frac{1}{k_m \partial_v} \qquad (5)$$

where k is the reaction rate, K is the intrinsic maximum reaction rate, L is the Langmuir adsorption coefficient, k_m is the mass diffusivity, and α_v is the surface to volume ratio. The equation suggests that part of the improvement in the reaction

rates are due to improved diffusivity. This can be seen if we divide the mass transport process into two steps. The first step is the chemical adsorption/desorption of the reactant/product on the semiconductor photocatalyst while the second is the diffusive process that removes the product from the surface into the bulk media and brings the reactants to the surface of the catalyst from the bulk media as shown in Fig. 1(b). While the process of chemical adsorption and desorption, most typically modeled by the Langmuir adsorption coefficient L, is determined by the chemical and material properties of the catalyst, the diffusive properties, modeled by k_m, can be greatly enhanced in a micro-optofluidic platform due to the presence of larger concentration gradients at even modest flow rates. Another feature that emerges is the high surface to volume ratio of these microreactors modeled by α_v. Indeed, previous studies have shown significant improvement in surface to volume ratios, whereas the surface to volume ratio would be 10 000–30 000 $m^2~m^{-3}$ in conventional reactors, they are <600 $m^2~m^{-3}$ in optofluidic reactors.[18] Fig. 2(c) shows an SEM of our thin film that shows the porous nature of the thin film.

From eqn (5) and the sorption times, one may construct a strategy to prescreen for potential catalysts which may benefit from an optofluidic platform. In particular, as long as the Langmuir adsorption rates are larger than the limiting rates given above and have demonstrated high bulk photocatalytic efficiencies, then the improvements in mass transfer efficiency and surface to volume ratios should have impact on the reaction rate. For iodide,[21] radiotracer measurements have shown the adsorption and desorption constants to be $6.90 \times 10^{-3}~min^{-1}$ to $3.68 \times 10^{-3}~min^{-1}$ and $2.56 \times 10^{-3}~min^{-1}$ to $3.69 \times 10^{-3}~min^{-1}$ respectively. For iodate,[22] relaxation techniques have found two different steps in the adsorption of this species onto TiO_2. Because one step is significantly slower than the latter, it is what is relevant for our purposes giving adsorption and desorption rates of $4.3 \times 10^3~mol^{-1}dm^3~s^{-1}$ and $2.0 \times 10~s^{-1}$, respectively. We suggest that a database

of efficient photocatalysts for this reaction along with their sorption rates could be used to screen for potential candidates.

Although, there might be significant improvement from better mass transport on the nanoscale, much of the improvements from increasing flow rates may have also been achieved by changing the device geometry. In particular, for the hydrogen-producing reaction, we found that for lower concentrations of iodide (20 μM NaI), the output yielded the equilibrium proportion concentration with 5% of iodide species catalyzed to iodate regardless of the flow rates. This means that some of the improvement was due to simply reducing the residence time of the reagents in the reactor and not necessarily due to better diffusion in microfluidic environments. Reducing the lifetime of the reactants in these reactors could have been achieved through other methods, for example, by simply decreasing the volume or area size of the reactor under the same flow rate and, therefore, the average time of the reagents in each reactor bed.

Conclusion

In this study, we have used for the first time, to our knowledge, a microfluidic platform to study photocatalytic water-splitting. We demonstrate how carrying out the reaction in an optofluidic environment significantly reduces the material costs and time associated with carrying out these reactions. We have used this platform to study the reaction kinetics of Pt–TiO$_2$ which we found agreed with previous literature. Additionally, we demonstrated that such platforms have the potential to enhance the reaction rates and efficiencies by improving mass transport. To this effect, we showed that simply increasing the flow rates yielded at least ∼2-fold improvements in reaction rates. We suggest that such an optofluidic platform could be used to rapidly and cheaply perform kinetic studies on different photocatalysts to screen for potential catalysts and optimize their reaction conditions.

Acknowledgements

References

1 D. L. Klass, *Biomass for Renewable Energy, Fuels, and Chemicals*, Elsevier Science, 1998.
2 O. Morton, *Nature*, 2006, **443**, 19–22.
3 J. M. Herrmann, *Catal. Today*, 1999, **53**, 115–129.
4 J. H. Mo, Y. P. Zhang, Q. J. Xu, J. J. Lamson and R. Y. Zhao, *Atmos. Environ.*, 2009, **43**, 2229–2246.
5 C. Wei, W. Y. Lin, Z. Zainal, N. E. Williams, K. Zhu, A. P. Kruzic, R. L. Smith and K. Rajeshwar, *Environ. Sci. Technol.*, 1994, **28**, 934–938.
6 A. Fujishima and K. Honda, *Nature*, 1972, **238**, 37–38.
7 A. Kudo and Y. Miseki, *Chem. Soc. Rev.*, 2009, **38**, 253–278.
8 H. Tong, S. X. Ouyang, Y. P. Bi, N. Umezawa, M. Oshikiri and J. H. Ye, *Adv. Mater.*, 2012, **24**, 229–251.
9 K. Maeda, M. Higashi, D. L. Lu, R. Abe and K. Domen, *J. Am. Chem. Soc.*, 2010, **132**, 5858–5868.
10 D. Erickson, D. Sinton and D. Psaltis, *Nat. Photonics*, 2011, **5**, 583–590.
11 L. Lei, N. Wang, X. M. Zhang, Q. D. Tai, D. P. Tsai and H. L. W. Chan, *Biomicrofluidics*, 2010, **4**, 043004.
12 J. W. Shi, J. T. Zheng, P. Wu and X. J. Ji, *Catal. Commun.*, 2008, **9**, 1846–1850.
13 L. Ge, M. X. Xu, M. Sun and H. B. Fang, *Mater. Res. Bull.*, 2006, **41**, 1596–1603.
14 Y. Ohko, A. Fujishima and K. Hashimoto, *J. Phys. Chem. B*, 1998, **102**, 1724–1729.
15 H. Lu, M. A. Schmidt and K. F. Jensen, *Lab Chip*, 2001, **1**, 22–28.
16 H. Lindstrom, R. Wootton and A. Iles, *AIChE J.*, 2007, **53**, 695–702.
17 R. Gorges, S. Meyer and G. Kreisel, *J. Photochem. Photobiol., A*, 2004, **167**, 95–99.
18 N. Wang, X. Zhang, B. Chen, W. Song, N. Y. Chan and H. L. W. Chan, *Lab Chip*, 2012, **12**, 3983–3990.
19 R. Abe, K. Sayama, K. Domen and H. Arakawa, *Chem. Phys. Lett.*, 2001, **344**, 339–344.
20 A. Galinska and J. Walendziewski, *Energy Fuels*, 2005, **19**, 1143–1147.
21 S. P. Mishra and N. Srinivasu, *Int. J. Radiat. Appl. Instrum., Part A*, 1992, **43**, 789–793.
22 K. Hachiya, M. Ashida, M. Sasaki, M. Karasuda and T. Yasunaga, *J. Phys. Chem.*, 1980, **84**, 2292–2296.